Ranking vocal fold model parameters by their influence on modal frequencies

Douglas D. Cook[a)]
School of Mechanical Engineering, Purdue University, 140 South Martin Jischke Drive, West Lafayette, Indiana 47907

Eric Nauman
Weldon School of Biomedical Engineering, Department of Basic Medical Science, Purdue University, 206 South Martin Jischke Drive, West Lafayette, Indiana 47907

Luc Mongeau
Department of Mechanical Engineering, McGill University, 817 Sherbrooke Street West, Montreal, Quebec H3A 2K6, Canada

(Received 19 January 2009; revised 26 June 2009; accepted 30 June 2009)

The purpose of this study was to identify, using computational models, the vocal fold parameters which are most influential in determining the vibratory characteristics of the vocal folds. The sensitivities of vocal folds modal frequencies to variations model parameters were used to determine the most influential parameters. A detailed finite element model of the human vocal fold was created. The model was defined by eight geometric and six material parameters. The model included transitional boundary regions to idealize the complex physiological structure of real human subjects. Parameters were simultaneously varied over ranges representative of actual human vocal folds. Three separate statistical analysis techniques were used to identify the most and least sensitive model parameters with respect to modal frequency. The results from all three methods consistently suggest that a set of five parameters are most influential in determining the vibratory characteristics of the vocal folds. © *2009 Acoustical Society of America.* [DOI: 10.1121/1.3183592]

PACS number(s): 43.70.Bk [AL] Pages: 2002–2010

I. INTRODUCTION

Highly detailed numerical models of human voice production are powerful tools for phonation research. Such models have been used, for example, to predict mechanical stresses and strains in vocal fold tissue (Gunter, 2003; Tao *et al.*, 2006; Tao and Jiang, 2007). Computational models are becoming more accurate and more realistic. It is anticipated that detailed finite element models, in conjunction with laboratory experiments, may yield a better understanding of the formation of polyps and nodules, vocal fold damage, and healing. Models may also be useful in evaluating potential prosthetic devices and in improving articulatory models for voice synthesis.

It is well known that vocal fold vibrations are highly affected by the elastic constants used to characterize the mechanical deformation of the vocal folds in detailed models (Alipour-Haghihi and Titze, 1985). Numerical simulations of phonation have demonstrated that variations in elastic constants can lead to chaos (Berry *et al.*, 1994) or biphonation (Tao and Jiang, 2006). The mechanical properties of vocal fold tissue may vary by orders of magnitude between subjects (Kakita *et al.*, 1981, Chan and Titze, 1999, Zhang *et al.*, 2006). Vocal fold geometry is similarly variable. Uncertainty in tissue and geometric parameters does contribute to overall model errors. A recent literature review of studies involving computational vocal fold models revealed that *ad hoc* estimates have been used for the majority of tissue parameter inputs in computational vocal fold models (Cook, 2009). Many tissue parameter estimates are used repeatedly throughout the literature with no rigorous verification. For example, one *ad hoc* estimate of the longitudinal shear modulus of the vocal ligament (40 kPa) has been used in most, if not all, previous studies. Considering the previously mentioned variability in vocal fold tissue parameter values, it is unlikely that this particular parameter has a unique value.

In general, the effects of tissue parameter uncertainty have not been investigated over the full range of plausible values in vocal fold models. While parametric methods have been used occasionally (Berry and Titze, 1996; Cook and Mongeau, 2007), this approach has not been widely adopted. Perhaps one reason is because systematic parametric studies are often prohibitively expensive, especially when fluid-structure interactions are modeled.

The purpose of the present study was to investigate the vibration response of a vocal fold model across a broad range of model parameters. The approach was based on principles of stochastic modeling: Parameter *ranges* were used rather than discrete values in order to obtain a broader understanding of the influence of structural parameters on vocal folds resonance frequencies. The objective was to identify the most and least sensitive model parameters. The underlying general hypothesis is that vocal fold models are insensitive to certain model parameters, moderately sensitive to others, and highly sensitive to a select group of parameters. Identifica-

[a)]Author to whom correspondence should be addressed. Electronic mail: ddcook@purdue.edu

 0001-4966/2009/126(4)/2002/9/$25.00

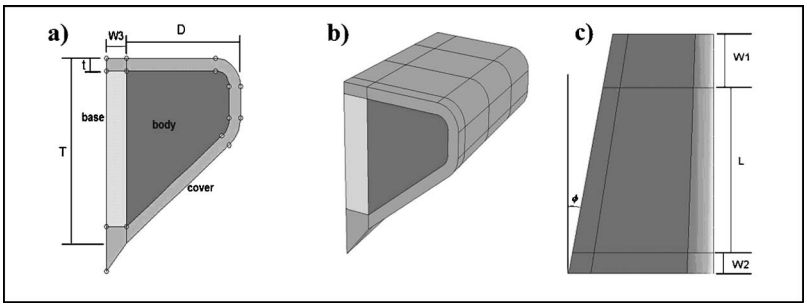

FIG. 1. Vocal fold model geometry: (a) coronal cross-section at the center of the mid-membranous region, (b) isometric view, and (c) superior view. Geometric symbol descriptions are listed in Table I.

tion and ranking of these parameters may provide valuable information for future model creation and may guide research in other areas where model complexity must be reduced. By focusing on the most sensitive parameters (and neglecting the least sensitive parameters), models may be created that are accurate and efficient while minimizing uncertainty. Furthermore, *a priori* confidence in such models may be enhanced when accounting for uncertainty over the broad parameter ranges found in vocal fold tissues.

II. VOCAL FOLD MODEL

A. Geometry

A three-dimensional body-cover model of the vocal folds was created after the two-layer models proposed by Hirano *et al.* (1981) and Story and Titze (1995). The vocal ligament was not assigned a distinct region but was assumed to be included as part of the cover. The model geometry was based on the two-dimensional M5 profile defined by Scherer *et al.* (2001). The cover was assumed to have a constant thickness over the medial, inferior, and superior surfaces. The two-dimensional coronal geometry [see Fig. 1(a)] was extruded in the anterior/posterior direction to obtain a three-dimensional geometry, as shown in Fig. 1(b). The depth (D) of the vocal fold decreased linearly from the anterior to the posterior ends to approximate the anterior/posterior asymmetry of the human vocal folds.

Vocal fold tissue has been reported to increase in stiffness toward the cartilage attachment points (Hirano *et al.*, 1987; Sataloff, 2005). Nearly all finite element vocal fold models (93%) have utilized the rigid rectangular boundary conditions of Titze and Strong (1975), with vocal fold tissue properties held constant throughout the structure. Hunter *et al.* (2004) questioned the accuracy of the rigid rectangular boundary conditions and used more realistic boundary conditions to investigate posturing of the vocal folds. Based on similar ideas, transitional boundary regions were added to both posterior and anterior of the vocal fold boundaries. The widths of these regions are labeled as W1, W2, and W3 in Fig. 1.

The paraglottic region (connective tissue lateral to the thyroarytenoid muscle and medial to the laryngeal cartilage (Hirano and Sato, 1993) was included in the model through the addition of an isotropic region at the base of the body region [indicated as "base" in Fig. 1(a)]. Rigid boundary conditions were applied on the anterior, posterior, and lateral faces, representative of the interface between the cartilages of the larynx and soft tissues of the vocal folds.

B. Material parameters

All tissues were modeled as incompressible. This approximation is commonly applied in vocal fold models and has been shown to introduce only minor errors in modal analysis (Cook *et al.*, 2008). The incompressibility assumption reduces the number of independent material parameters required to define the elastic properties of each tissue region. All tissues were assumed to be linearly elastic for the same reasons set forth in the previous reference.

The behavior of isotropic tissues is entirely defined by Young's modulus, E. Incompressible transversely isotropic tissues are defined by three material parameters: the transverse Young's modulus (E), the longitudinal Young's modulus (E'), and the longitudinal shear modulus (G'). The same density was assumed for all tissue types.

The vocal fold model was divided into seven regions, each with distinct material parameters. The vocal fold body and cover included anterior, mid-membranous, and posterior regions for a total of six regions. The seventh region was the paraglottic region. The cover regions and the paraglottic region were modeled as isotropic, with the body regions modeled as transversely isotropic.

All parameter values were assumed to be constant within the mid-membranous regions. Tissue parameters were assumed to vary continuously between the mid-membranous region and anterior or posterior faces. Although the cartilage was not explicitly modeled, the tissue property values at anterior and posterior faces of the model were representative of cartilage tissue. The spatial variation in all independent tissue parameters was determined as

$$S_{x/\mathrm{ant}} = S_{x/\mathrm{mid}} + (S_{\mathrm{cart}} - S_{x/\mathrm{mid}})\left(\frac{x - L - w_2}{w_1}\right)^P, \tag{1}$$

$$S_{x/\mathrm{pos}} = S_{x/\mathrm{mid}} + (S_{\mathrm{cart}} - S_{x/\mathrm{mid}})\left(\frac{w_2 - x}{w_2}\right)^P. \tag{2}$$

In these equations, $S_{x/\mathrm{ant}}$ and $S_{x/\mathrm{pos}}$ represent the varied parameter S_x in the anterior and posterior boundary regions, respectively. The corresponding cartilage value is S_{cart}, and the parameter value at the mid-membranous region is $S_{x/\mathrm{mid}}$. The equation for the variation of the cover stiffness in the anterior region was

$$E_{c/\mathrm{ant}} = E_c + (E_{\mathrm{cart}} - E_c)\left(\frac{x - L - w_2}{w_1}\right)^P. \tag{3}$$

A similar relation was used for other material parameters: E_c, E_b, E', and G'.

TABLE I. Parameter descriptions, symbols, ranges, and references. The first eight parameters refer to the model geometry; the last seven refer to material properties.

Parameters	Symbol	Range	Reference
Length	L	6.8–10.2 mm	Friederich *et al.*, 1993; Titze, 2006
Depth	D	7–10 mm	Estimated
Thickness	T	5.9–8.8 mm	Titze, 2006
Cover thickness	t	0.84–1.26 mm	Titze, 2006; Stiblar-Martincic, 1997
Angle	φ	0°–28°	Estimated
Length of W 1	W1	3.6–5.4 mm	Friederich *et al.*, 1993
Length of W 2	W2	1.0–1.6 mm	Friederich *et al.*, 1993
Depth of W 3	W3	1.6–2.4 mm	Inferred from Hirano and Sato, 1993
Cover stiffness	E_c	4–50 kPa	Zhang *et al.*, 2006
Transverse Young's modulus	E_b	1–30 kPa	de Vries *et al.*, 1999; Gunter, 2003
Longitudinal Young's modulus	E'	E_b–E_{cart}	E_b and E_{cart}
Stiffness of W3	E_{base}	50–1000 kPa	Estimated
Longitudinal shear modulus	G'	5–100 kPa	Rosa *et al.*, 2003; Berry and Titze, 1996
Degree of transition function	P	1–66	Estimated
Cartilage Young's modulus	E_{cart}	10 MPa (fixed)	Rains *et al.*, 1992; Roberts *et al.*, 1998

For all isotropic regions, Poisson's ratio was held constant, $\upsilon=\frac{1}{2}$, and the shear modulus varied as a function of local stiffness. For example, in the case of cover shear modulus,

$$G_{c/\text{ant}} = \frac{E_{c/\text{ant}}}{2(1+\nu)}, \tag{4}$$

$$G_{c/\text{pos}} = \frac{E_{c/\text{pos}}}{2(1+\nu)}. \tag{5}$$

For transversely isotropic regions, the shear modulus varied as a function of (local) longitudinal and transverse Young's modulus values,

$$\mu = \frac{E_b E'}{4E' - E_b}. \tag{6}$$

The Poisson's ratios also varied spatially according to the following equations:

$$\nu' = \tfrac{1}{2}, \tag{7}$$

$$\nu^{+} = \frac{E}{2E'}, \tag{8}$$

$$\nu = 1 - \frac{E}{2E'}. \tag{9}$$

The above methods allowed the tissue stiffness, Poisson's ratios, and shear moduli to vary continuously between the mid-membranous region and the cartilage values at the anterior and posterior surfaces. The independent parameters governing these transitions were the mid-membranous material parameters (E_c, E_b, E', G'), the cartilage tissue parameter (E_{cart}), and the exponent P which controlled the rate of transition between regions.

1. Parameter ranges

The vocal fold model described above is defined by eight geometric and seven material (tissue) parameters. To obtain a robust description of the vocal fold structure, parameter ranges were established for all independent parameters based upon available measured data or *ad hoc* estimates. The guiding principle in the range selection was to encompass approximately 75% of human vocal fold values.

For example, the medial/lateral thickness of the vocal folds was reported by Titze (2006) as having a mean value of 9.34 mm with a standard deviation of 1.63 mm. Assuming a normal distribution, 75% of vocal fold thicknesses should lie between 5.87 and 8.81 mm. When mean and standard deviation values were not available, *ad hoc* estimates based on experimental data from measurements of similar tissues or previous vocal fold models were used.

Vocal fold tissues are known to exhibit nonlinear stress-strain relationships (Chan and Titze, 1999; Zhang *et al.*, 2006). Nonlinear relations are available for only a few of the parameters identified in Sec. II B. The use of nonlinear constitutive models requires additional model parameters, most of which are extremely difficult or impossible to estimate. This problem was addressed by choosing linear material parameters over ranges that were sufficiently broad to encompass both zero strain and moderate (i.e., 10%–15%) strain parameter values. All geometric and material parameters, with their associated ranges, are listed in Table I.

C. Numerical implementation

This study employed more than 2000 unique vocal fold models. The commercial finite element software COMSOL, along with MATLAB Version 3.4 was used. A custom subroutine created each finite element model based on unique sets of 14 parameters (Table I). For each set of parameters, a vocal fold geometry was defined, tissue properties were assigned, a finite element mesh was created, boundary conditions were imposed, and modal analysis was performed. The output consisted of eight unique eigenvectors and eight associated eigenvalues or resonance frequencies. Eigenvectors contained the x-, y-, and z-displacement values for each node.

TABLE II. Modal analysis comparisons for three different methods. Rightmost column indicates the maximum percent difference between COMSOL predictions and the remaining two methods.

Mode	Mode shape[a]	Modal frequency (Hz)			Maximum difference
		Experimental	ABAQUS	COMSOL	
1	z-10	75	74.17	74.52	−6.9%
2	z-20	···	106.55	107.08	0.50%
3	y-10	···	125.57	125.67	0.08%
4	*x*-10	···	133.99	134.63	0.48%
5	*x*-11	···	150.38	150.91	0.35%
6	*x*-20	···	151.32	152.08	0.50%

[a]Mode shape convention: Berry *et al.* (1994).

For each vocal fold model, the mesh consisted of approximately 1500 quadratic finite elements with over 28 000 degrees of freedom. A mesh refinement study was performed to verify spatial convergence. The model was validated through comparisons with measured data for a synthetic physical model of the vocal folds (Chen *et al.*, 2008). The synthetic model geometry was similar to that of the model described above, with a single isotropic layer and no transitional boundary regions. Due to high damping in the synthetic model, experimental modal analysis results were obtained for only the first mode of vibration. Computational modal analysis was also performed using the commercial software package ABAQUS. The experimental studies and ABAQUS simulations were performed independently. Table II provides comparisons between these methods. Very good agreement was found between the COMSOL and ABAQUS models, both of which adequately predicted the experiment.

III. DATA ANALYSIS TECHNIQUES

Three different techniques were applied in the analysis of the output data. The first was a screening method, as set forth by Cotter (1979). The second examined the correlation between parameter values and modal frequencies. The final method was based on descriptive statistics of 100 local sensitivity simulations. These methods are described in Secs. III A–III C.

A. Cotter's method

So-called screening methods are one class of methods used to perform sensitivity analysis (Saltelli *et al.*, 2000). Screening methods provide a ranking of model parameters based on the importance or influence of each parameter on the overall model response. Screening methods utilize a limited number of simulations to reduce computational cost but occasionally fail to identify key parameters and cannot precisely quantify the contribution of each parameter. These methods yield essentially first-order estimates of each parameter's importance.

The method proposed by Cotter (1979) involves $2n+2$ total simulations, where n is the number of model parameters. A two-level factorial design was used with all parameter values set to their highest or lowest value. The first simulation (case zero) is performed with all parameters set to low values. The final simulation is performed with all parameters set to high values. Cases 1 through n are based on the zero case with all parameters at their lowest values and with one parameter at a time set to its highest value. Cases $(n+1)$ through $2n$ are variations of the final case with one parameter at a time set to its lowest value.

Cotter provided a method for estimating the importance of each factor based on the $2n+2$ simulation outputs designated as y_i. The relative importance of the jth parameter, $M(j)$, is given by

$$M(j) = |y_{2n+1} - y_{n-j} + y_j - y_0| + |y_{2n+1} - y_{n+j} - y_j - y_0|. \tag{10}$$

The leftmost absolute value term quantifies the effect of varying only one parameter at a time. The second (right) absolute value term accounts for interaction effects.

B. Correlation between modal frequencies and model parameters

The ranges given in Table I were used to define uniform probability density functions (PDFs) for each parameter. Vocal fold models were created by randomly selecting each parameter from its corresponding distribution. A total of 100 vocal fold models were created in this fashion $(n=100)$. Pearson correlations were used to determine possible relationships between simulation outputs (modal frequencies) and each of the input parameters. The correlation coefficient, r_{ij}, was calculated for each of the first eight modal frequencies (subscript i) and for each of the 14 input parameters (subscript j). This yielded 112 total correlation values. The coefficient of determination (r^2) was also calculated. Finally, p-values were obtained via a hypothesis test. The null hypothesis (H_0) was that no relationship existed between modal frequencies and parameter values $(H_0: r=0)$. The alternative hypothesis is that modal frequencies and model parameters were correlated with an r-value greater than or equal to each respective r_{ij}-value $(H_A: r \geq r_{ij})$. The test statistic was $t=(n-2)r^2/(1-r^2)^{1/2}$, which follows a standard t-distribution. Since the alternative hypothesis was that $r \geq r_{ij}$, a one-sided t-distribution was used for determination of p-values.

C. Local sensitivity analysis

The final analysis method involved computing local sensitivity values for each mode and parameter. The local sensitivity of each modal frequency, M_i, to each parameter, X_j, was defined as the partial derivative,

$$S_{ij} = \frac{\partial M_i}{\partial X_j}. \tag{11}$$

The sensitivity, S_{ij}, was evaluated using a finite difference approximation. First, a nominal case, M^{nom}, was randomly selected, and its modal frequencies were calculated. Next, each parameter X_j was increased slightly, with all other parameters held at their nominal values. Finally, the sensitivity to each modal frequency was computed as

$$S_{ij} = \frac{\partial M_i}{\partial X_j} \approx \frac{M_i' - M_i^{\text{nom}}}{X_j' - X_j^{\text{nom}}}, \tag{12}$$

where the nom superscript refers to nominal values and the primed quantities are associated with incremented X_j values.

The units of the sensitivity depend upon the parameter of interest. To allow comparison between sensitivities of different parameters, each parameter was non-dimensionalized as follows:

$$X_j^* = \frac{X_j}{R_j}, \tag{13}$$

where R_j refers to the range of parameter j. Using P_j^*, the sensitivity was expressed as

$$S_{ij} = \frac{\partial M_i}{\partial X_j^*} \approx \frac{M_i' - M_i^{\text{nom}}}{(X_j' - X_j^{\text{nom}})/R_j}. \tag{14}$$

This sensitivity can be interpreted as the change in modal frequency due to a unit percent change in parameter j. This approach was used to obtain 112 total sensitivities for each nominal case. The sample of 100 vocal fold models used for correlation analysis was used as the nominal set, with sensitivities calculated for each unique model. This process required the creation of 1500 individual vocal fold models (100 nominal cases, with 1400 additional cases required for sensitivity calculations). The computational time was approximately 16 h using two (dual) 2.2 GHz XEON processors with 1 Gbyte random access memory.

IV. RESULTS

A. Cotter's method

Cotter's method yields a single importance value for each parameter-mode pair for a total of 112 importance values. Importance values were observed to depend primarily on each parameter, with no apparent dependence on modal frequency. Importance value statistics are presented in Table III for each parameter, with distributions of importance values indicated by their standard deviation as well as their maximum and minimum values.

Cotter's method identified the cover stiffness, E_c, as the most important parameter, followed by P, G', E_b, and L. The five least important parameters were identified as W1, t, φ, W2, and W3. The importance values for individual modes were remarkably consistent among the five most important parameters. In fact, 85% of individual importance values from the lead group were greater than the highest importance value found in the remaining nine parameters. A similar consistency was found among the five least important parameters.

TABLE III. Importance values obtained from Cotter's method. Each row based upon eight parameter-modal frequency pairs ($n=8$).

	Importance value statistics			
Parameter	Mean (st. dev)		Max/min	Rank
L	21.03	(5.40)	31.5/16.1	5
D	19.23	(1.63)	21.9/17.6	6
T	8.85	(2.53)	13.0/3.8	9
t	5.99	(2.54)	9.9/2.7	11
φ	5.15	(2.05)	9.4/2.9	12
W1	7.47	(2.58)	12.0/4.2	10
W2	2.93	(0.70)	4.0/2.2	13
W3	1.79	(0.41)	2.7/1.4	14
E_c	54.14	(14.9)	74.9/33.1	1
E_b	31.07	(8.17)	40.2/15.8	4
E'	13.62	(6.30)	23.6/3.4	7
E_{base}	9.09	(2.48)	12.6/5.8	8
G'	33.20	(6.21)	42.5/24.6	3
P	35.56	(5.84)	44.7/30.2	2

B. Correlation results

For a sample size of 100 models, Pearson correlation coefficients, r_{ij}, coefficients of determination, $(r_{ij})^2$, and p-values were calculated. A total of 112 values were obtained for each of these three statistical coefficients. The results were again primarily dependent on parameter values, with little dependence on mode number. Means, standard deviation, maximum, and minimum values are reported for the data corresponding to each parameter in Table IV. The Pearson correlation coefficients ranged from $r_{3,14}=-0.45$ to $r_{8,12}=0.60$. The absolute values of correlation coefficients ranged from $r_{4,7}=0.0047$ to $r_{8,12}=0.60$. The mean and standard deviations of r-values for all modes are given in Table IV. Positive r-values indicate that the parameters are positively correlated with modal frequency, while negative values indicate negative correlations. Although r-values were much lower than typically encountered in engineering experiments, statistical significance was due to a large number of degrees of freedom (df=99).

The five most correlated with model frequency were E_c, E_b, P, G', and L. The five parameters least correlated with modal frequency were φ, E', t, W2, and W1. As expected, tissue stiffness parameters typically showed a positive correlation with modal frequency, while geometric parameters tended to have a negative correlation. Some exceptions to these generalizations included E', which had a weak negative correlation, as well as T and t, which exhibited weakly positive correlations.

The r^2-values can be interpreted as the percentage of variation in modal frequency associated with each parameter.

TABLE IV. Statistics of r, r^2, and p-values. Means and standard deviations were based on the eight modal frequency values for each parameter. Values in bold highlights the r, r^r, and p-values of significantly correlated parameters.

	r-values			r^2-values			p-values			
Parameters	Mean (st. dev)		Max/min	Mean (st. dev)		Max/min	Mean (st. dev)		Max/min	Rank
L	**−0.27**	(0.03)	−0.24/−0.31	**0.08**	(0.02)	0.10/0.06	**0.004**	(0.00)	0.007/0.001	**5**
D	**−0.20**	(0.02)	−0.17/−0.22	**0.04**	(0.01)	0.05 /0.03	**0.027**	(0.01)	0.044/0.013	**7**
T	0.09	(0.05)	0.15/0.02	0.01	(0.01)	0.02 /0.00	0.211	(0.13)	0.412/0.070	10
t	0.04	(0.03)	0.07/−0.01	0.00	(0.00)	0.01 /0.00	0.354	(0.09)	0.477/0.234	12
φ	−0.09	(0.03)	−0.05/−0.13	0.01	(0.01)	0.02 /0.00	0.198	(0.08)	0.296/0.094	9
W1	0.00	(0.01)	0.02/−0.01	0.00	(0.00)	0.00 /0.00	0.458	(0.03)	0.498/0.430	14
W2	0.02	(0.01)	0.03/0.00	0.00	(0.00)	0.00 /0.00	0.429	(0.04)	0.482/0.375	13
W3	**−0.23**	(0.02)	−0.20/−0.26	**0.05**	(0.01)	0.07 /0.04	**0.012**	(0.00)	0.020/0.005	**6**
E_c	**0.55**	(0.04)	0.60/0.50	**0.30**	(0.04)	0.36 /0.25	**0.000**	(0.00)	0.000/0.000	**1**
E_b	**0.44**	(0.05)	0.54/0.38	**0.20**	(0.05)	0.29 /0.14	**0.000**	(0.00)	0.000/0.000	**2**
E'	−0.07	(0.02)	−0.05/−0.09	0.01	(0.00)	0.01 /0.00	0.245	(0.06)	0.324/0.181	11
E_{base}	0.11	(0.02)	0.13/0.08	0.01	(0.00)	0.02 /0.01	0.141	(0.04)	0.202/0.095	8
G'	**0.31**	(0.03)	0.35/0.27	**0.09**	(0.02)	0.13 /0.07	**0.001**	(0.00)	0.003/0.000	**4**
P	**−0.38**	(0.04)	−0.35/−0.45	**0.15**	(0.03)	0.20 /0.12	**0.000**	(0.00)	0.000/0.000	**3**

This suggests that approximately 30% of the modal frequency variation is due to E_c, with E_b, P, G', and L contributing 20%, 15%, 9%, and 8%, respectively.

p-values were also calculated to test the null hypothesis that no relationship existed between parameters and modal frequencies. Seven parameters possessed p-values lower than 0.025, with the majority of p-values in this group lower than 0.001. For these parameters, the null hypothesis was rejected in favor of the alternative hypothesis. Several parameters had p-values greater than 0.025, indicating a non-negligible possibility that the null hypothesis may be true. These parameters included T, t, φ, W1, W2, E', and E_{base}.

C. Local sensitivity results

As described in Sec. III C, a total of 11 200 total local sensitivities were calculated. These sensitivities were then grouped into 800 sensitivities for each parameter. The absolute value of the 10% trimmed mean was chosen to rank parameter influence since this value is more moderate than either the mean or median. The most sensitive parameters were P, E_c, G', E_b, and L. The least sensitive parameters were T, E_{base}, W2, φ, and W3.

The model parameters are grouped into geometric (L, D, T, t, φ, W1, W2, and W3) and tissue parameters (E_c, E_b, E', E_{base}, and G'). The *signs* of the 10% trimmed mean values reveal some expected characteristics of the model. For tissue parameters, all mean sensitivity values were positive, and 99.8% of all sensitivities associated with these parameters were also positive. This is in agreement with expectations that an increase in stiffness increases modal frequency. Geometric parameters typically exhibited negative local sensitivities, as expected, with 80% of geometric sensitivities below zero. Although increased mass typically reduces modal frequencies, geometric parameters also influence the model stiffness through boundary conditions. Tradeoffs between added mass and added boundary area vary, thus causing some geometric parameters such as thickness and extrusion angle to have positive trimmed means. The same effect is responsible for the slight positive (but insignificant) correlations observed for certain geometric parameters (see Table IV).

A high sensitivity to the rate of transition in the transitional boundary regions (P) was observed. Low values of P caused the boundary effects to extend further inward from each fixed boundary. For high values, the boundary regions act as extensions of the mid-membranous region, thus effectively lengthening the vibrating length of the vocal folds.

D. Comparison between methods

The three methods utilized are not directly comparable. Each relies upon different assumptions, incorporates different amounts of data, and produces different rankings. However, the methods can be compared in a relative sense. To this end, the results of each method were normalized by the sum of all primary results. This approach preserves relative importance within each method while allowing the various rankings to be compared with each other. For example, the trimmed mean values of Table V were summed, after which each individual value was divided by the sum. Similar approaches were used for the mean values of Table III and the r-values of Table IV. The results are shown graphically in Fig. 2 below. The parameters were ordered along the ordinate axis according to the average of each parameter's three normalized values.

As seen in Fig. 2, the three methods are in general agreement, but they do not always agree. The most obvious differences are observed for P and W3. The P parameter was consistently ranked among the top 5 but exhibited an unusually high value from the local sensitivity method. This seems due to the fact that the model was observed to be extremely sensitive to low values of P (i.e., 1–5), and less sensitive to values above 5. The third transitional boundary region (W3) was identified as the sixth most influential parameter by the correlation method, whereas both Cotter's method and the local sensitivity approach ranked this parameter among the least sensitive parameters. These discrepancies may be due

TABLE V. Statistics for local sensitivity values. Each row is based upon local sensitivity values ($n=800$).

Parameters	Local sensitivity statistics			
	Mean (st. dev)	Trimmed mean	Median	Rank
L	−48.63 (20.3)	−50.7	−51.6	5
D	−13.10 (9.64)	−14.1	−14.9	6
T	7.17 (10.9)	7.0	6.8	10
t	−6.30 (11.0)	−7.1	−7.9	9
φ	1.55 (57.3)	2.4	4.6	13
W1	−11.70 (6.97)	−12.0	−12.3	7
W2	−3.51 (4.15)	−3.6	−3.8	12
W3	−0.92 (3.91)	−1.1	−1.4	14
E_c	75.66 (58.7)	81.3	85.3	2
E_b	47.38 (97.9)	55.4	61.9	4
E'	4.18 (159.)	8.4	29.0	8
E_{base}	2.88 (48.9)	5.0	8.1	11
G'	49.33 (82.0)	60.4	65.2	3
P	−310.9 (387)	−362.7	−395.6	1

to sample size, the choice of parameter ranges, or unidentified interaction effects with other parameters. The general agreement between methods, especially concerning the most sensitive parameters, was judged to be more compelling than the discrepancies.

V. DISCUSSION

A. Difficulty in mode shape identification

The mode shapes of the human vocal folds are often described using the x-10, x-11 nomenclature of Titze and Strong (1975). These mode shapes take on different modal frequencies depending upon model parameters, and modal frequencies have been shown to cross as model parameters are varied [see Berry and Titze (1996), Fig. 3]. Because eigenvalue solvers generally order results according to increasing modal frequency, eigenvectors (mode shapes) are not immediately differentiable based on modal frequencies alone. For example, the x-11 mode might appear as the third eigenvector for one set of model parameters but as the fourth eigenvector for a different set of model parameters.

With hundreds of distinct models created over the course of this study, mode shape identification was a major challenge. Simultaneous variation in all model parameters over broad ranges exacerbated this problem, leading to high variance in modal frequencies. It was observed that the PDF of modal frequencies for any given mode shape exhibited substantial overlap with the PDFs of other mode shapes. An analogous situation was also observed in the eigenvector space. Although all finite element models had the same mesh (to allow eigenvector comparisons), eigenvectors exhibited a high level of variance, making mode shape identification difficult. Several comparative schemes were attempted but produced unacceptable rates of false-positive and/or false-negative identifications.

Because of this difficulty, the modal frequencies were analyzed as obtained from the eigenvalue solver (i.e., ordered by modal frequency). It was anticipated that this approach would have a moderating effect on analysis outcomes since highly sensitive mode shapes would occasionally be combined with less sensitive ones, and vice versa. For the purposes of identifying the most and least sensitive parameters at first-order accuracy, this shortcoming was deemed acceptable. The general agreement between the three analysis methods suggests that this approach was justified.

B. Variation in model parameters in relation to previous models

Cook (2009) reported that the average number of parameters for vocal fold models was 20 with an average of three parameters varied in each study. Of the tissue parameters used in this study (E_c, E_b, E', and G'), an average of five unique parameter values have been reported in the literature (Cook, 2009). While this figure is certainly an underestimate (many values were found to be unreported), the present study utilized over 100 unique values for each of 14 parameters. All parameters were varied simultaneously, thus allowing for a broader sampling of the entire parameter space than can be obtained by varying one parameter at a time as is typically

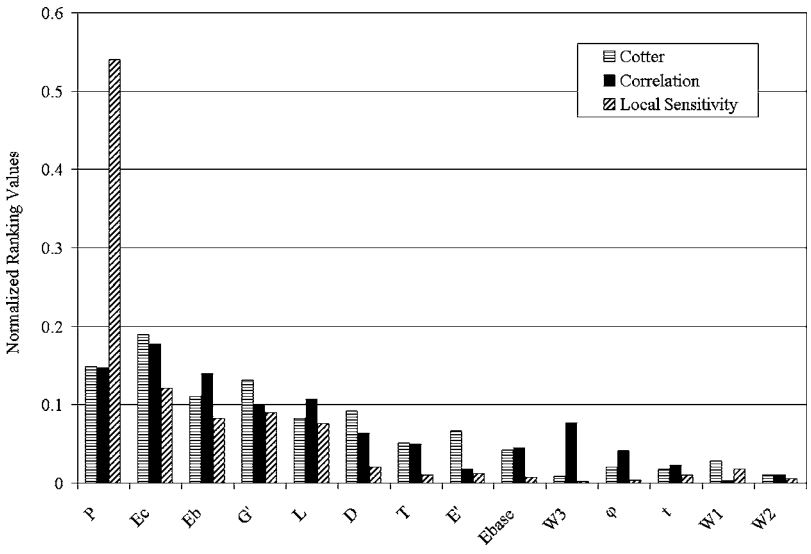

FIG. 2. Normalized ranking values for comparison between methods.

done. As such, the models described in this study account for more variation in vocal fold structure than all previous computational vocal fold studies combined.

C. Discussion of results

The reliability of the results presented above is partially dependent on the number of data points utilized by each method. Cotter's method relied upon 240 total modal frequency values, while the correlation and local sensitivity approaches utilized 800 and 11 200 modal frequencies, respectively. From this perspective, the latter two approaches are more reliable since they provide more comprehensive descriptions of how the model behaves across the entire spectrum of possible parameter combinations.

The most striking feature observed in the application of these three methods was the consistency with which the lead group of parameters, consisting of E_c, P, E_b, G', and L, were identified as influential on modal frequencies. Four of these parameters are related to tissue properties, and only one parameter (L) is a geometric parameter. There are two reasons for identifying these *five* parameters as the most sensitive. First, each of these parameters was ranked within the top five by each of the three methods of analysis. Second, certain parameters known from prior research to strongly influence vocal fold vibration should be expected to appear among the group of most sensitive parameters. Such parameters included the stiffness of the vocal fold cover (E_c) and vocal fold length (L). The mechanical properties of the cover are known to be a dominant factor in healthy phonation (Chan and Titze, 1999). Vocal fold length has been attributed to the difference between male and female fundamental frequencies of phonation (Friederich *et al.*, 1993; Perkins and Kent, 1986). Finally, the presence of E_c and L among the most sensitive parameters indicates the importance of the remaining parameters, all of which were observed to be more influential than the vocal fold length.

The least sensitive parameter ratings were less consistent than the most sensitive parameters. The parameters W1, W2, and t appeared among the five least sensitive parameters for each method. The vocal fold thickness (T) was ranked 9th, 10th, and 10th by the three respective methods. The longitudinal body stiffness (E') was ranked as 11th by both regression and correlation methods but was ranked 7th by Cotter's method. Both T and E' were included with the least sensitive parameters based on their consistently low ranking by both correlation and local sensitivity approaches. Thus, the five least sensitive parameters were found to be T, E', t, W1, and W2.

It is difficult to make any definitive statement about the remaining parameters (D, W3, E_{base}, and φ). Some of these parameters (such as D) may have a substantial influence on the dynamic response of the vocal folds, while others (such as E_{base}) may have little influence. More advanced analysis, involving fluid loading of the vocal fold structure and/or sorting of modal frequency data, will be required to provide a more accurate ranking of these parameters.

D. Application of results

The above results have several interrelated applications. First, these results can be used to guide the experimental measurement of vocal fold tissues. The measurement of highly sensitive parameters should be prioritized over the measurement of less sensitive parameters. Furthermore, sensitive parameters require both more accurate and more comprehensive measurements than less sensitive parameters. In other words, the ranges, distributions, and gender- and age-dependent relationships of highly sensitive parameters should be characterized with greater detail.

Second, the identification of the most and least sensitive model parameters has great importance for computational models of phonation. Models should be created with all parameter sensitivities in mind. This is a double-edged issue. On one hand, the identification of non-influential parameters allows those parameter values to be chosen with relative impunity since these choices will have little effect of model response. On the other hand, a great deal of care and attention must be paid to highly sensitive model parameters, many of which have not yet been characterized in sufficient detail. In fact, previous models of phonation have typically utilized *ad hoc* estimates for several of the most sensitive material parameters (Cook *et al.*, 2009) in review, supplemental document]. Highly sensitive parameters should either be based on experimental data or varied parametrically to account for uncertainty until more such data are available.

Third, the ranking of model parameters may be useful in the creation of patient-specific models of phonation and (indirectly) in the evaluation of individuals suffering from voice disorders. Based on the ranking presented above, the least sensitive parameters would be based on general population trends, and even some moderately sensitive parameters could be estimated. However, a sufficiently accurate patient-specific model would require patient-specific data for the most sensitive vocal fold parameters. The achievement of patient-specific models will undoubtedly require a great deal of research focused on methods for obtaining *in vivo* measurement of the most sensitive parameter values. The ranking of model parameters provides some guidance on this front, suggesting which parameters should be targeted initially. This issue is related to the characterization of parameter distributions. For example, detailed experimental characterization of vocal fold parameters may reveal that certain parameters (such as P), although highly influential, exhibit relatively narrow distributions and thus may be estimated without introducing a great deal of error in the analysis.

Finally, the identification of several highly influential parameters may suggest new approaches for treating certain voice disorders, especially thyroplasty implants and injections. For example, vocal fold medialization implant designs could be improved to mimic the most influential human vocal fold characteristics as reported above. New medialization injection materials could also be developed to exhibit sensitivities similar to those of the actual human vocal folds. Both approaches would utilize a more complete understanding of the human vocal fold structure to create treatments that restore functionality of the human voice.

VI. CONCLUSIONS

The application of three separate methods was used to identify the most and least sensitive parameters of a vocal fold model. All three methods identified the following parameters as most sensitive: the stiffness of the cover (E_c), the stiffness of the body (E_b), the rate of transition between midmembranous and cartilage stiffness (P), the longitudinal shear stiffness of the body (G'), and the vocal fold length (L). The least sensitive model parameters included the following (in descending order): E', T, t, W1, and W2. Moderately sensitive parameters were identified as D, W3, E_{base}, and φ. Such ranking of vocal fold parameters is useful to guide (a) experimental measurements and characterization of vocal fold parameters, (b) the creation of accurate computational models of phonation in general, (c) the development of techniques for obtaining patient-specific models of phonation, and (d) further improvements in the treatment of voice disorders.

ACKNOWLEDGMENTS

The authors gratefully acknowledge financial support from the National Institute on Deafness and Other Communication Disorders (Grant Nos. R01 DC005788 and R01 DC008290), the National Science Foundation (Grant No. CBET-0828903), and the ASME Teaching Fellowship. Li-Jen Chen graciously provided experimental and computational modal analysis results for validation of the models in this study. Portions of this paper were originally presented at the 6th International Congress on Voice Physiology and Biomechanics in Tampere, Finland 6–9 August 2008.

Alipour-Haghihi, F., and Titze, I. R. (**1985**). "Simulation of particle trajectories of vocal fold tissue during phonation," in *Vocal Fold Phyisiology: Biomechanics, Acoustics, and Phonatory Control*, edited by I. R. Titze and R. S. Scherer (Denver Center for the Performing Arts, Denver), pp. 183–190.

Berry, D. A., Herzel, H., Titze, I. R., and Krisher, K. (**1994**). "Interpretation of biomechanical simulations of normal and chaotic vocal fold oscillations with empirical eigenfunctions," J. Acoust. Soc. Am. **95**, 3595–3604.

Berry, D. A., and Titze, I. R. (**1996**). "Normal modes in a continuum model of vocal fold tissues," J. Acoust. Soc. Am. **100**, 3345–3354.

Chan, R. W., and Titze, I. R. (**1999**). "Viscoelastic shear properties of human vocal fold mucosa: Measurement methodology and empirical results," J. Acoust. Soc. Am. **106**, 2008.

Chen, L. J., Zanartu, M., Cook, D., and Mongeau, L. (**2008**). "Effects of acoustic loading on the self-oscillations of a synthetic model of the vocal folds," Proceedings of the Ninth International Conference on Flow-Induced Vibration, Prague, Czech Republic, 30 June–3 July, edited by I. Zolotarev and J. Horacek.

Cook, D. D. (**2009**). "Systematic structural analysis of human vocal fold models," Ph.D. dissertation, Purdue University, IN.

Cook, D. D., and Mongeau, L. (**2007**). "Sensitivity of a continuum vocal fold model to geometric parameters, constraints, and boundary conditions," J. Acoust. Soc. Am. **121**, 2247–2253.

Cook, D. D., Nauman, E., and Mongeau, L. (**2008**). "Reducing the number of vocal fold mechanical tissue properties: Evaluation of the incompressibility and planar displacement assumptions," J. Acoust. Soc. Am. **124**, 3888–3896.

Cotter, S. C. (**1979**). "A screening design for factorial experiments with interactions," Biometrika **66**, 317–320.

de Vries, M., Schutte, H., and Verkerke, G. (**1999**). "Determination of parameters for lumped parameter models of the vocal folds using a finite-element method approach," J. Acoust. Soc. Am. **106**, 3620–3628.

Friedrich, G., Kainz, J., and Freidl, W. (**1993**). "Zur funktionellen strucktur der menschlichen stimmlippe (Functional structure of the human vocal cord)," Laryngorhinootologie **72**, 215–224.

Gunter, H. (**2003**). "A mechanical model of vocal-fold collision with high spatial and temporal resolution," J. Acoust. Soc. Am. **113**, 994–1000.

Hirano, M., Kurita, S., and Nakashima, T. (**1981**). "The structure of the vocal folds," in *Vocal Fold Physiology*, edited by K. Stevens and M. Hirano (University of Tokyo, Tokyo), pp. 33–41.

Hirano, M., and Sato, K. (**1993**). *Histological Color Atlas of the Human Larynx* (Singular Publishing Group, San Diego, CA).

Hirano, M., Yoshita, T., Kurita, S. Kiyokawa, K., Sato, K., and Tateishi, O. (**1987**). "Anatomy and behavior of the vocal process," in *Laryngeal Function in Phonation and Respiration*, edited by T. Baer, C. Sasaki, and K. Harris (College-Hill, Boston, MA), pp. 1–13.

Hunter, E. J., Titze, I. R., and Alipour, F. (**2004**). "A three-dimensional model of vocal fold abduction/adduction," J. Acoust. Soc. Am. **115**, 1747–1759.

Kakita, Y., Hirano, M., and Ohmaru, K. (**1981**). "Physical properties of the vocal fold tissue," in *Vocal Fold Physiology*, edited by K. Stevens and M. Hirano (University of Tokyo, Tokyo, Japan).

Perkins, W., and Kent, R. (**1986**). *Functional Anatomy of Speech, Language, and Hearing: A Primer* (Allyn and Bacon, Boston, MA).

Rains, J. K., Bert, J. L., Roberts, C. R., and Pare, P. D. (**1992**). "Mechanical properties of human tracheal cartilage," J. Appl. Physiol. **72**, 219–225.

Roberts, C. R., Rains, J. K., Pare, P. D., Walker, D. C., Wiggs, B., and Bert, J. L. (**1998**). "Ultrastructure and tensile properties of human tracheal cartilage," J. Biomech. **31**, 81–86.

Rosa, M. O., Pereira, J. C., Grellet, M., and Alwan, A. (**2003**). "A contribution to simulating a three-dimensional larynx model using the finite element method," J. Acoust. Soc. Am. **114**, 2893–2905.

Saltelli, A., Chan, K., and Scott, E. M. (**2000**). *Sensitivity Analysis* (Wiley, Chichester, NY).

Sataloff, R. T. (**2005**). *Voice Science* (Plural Publishing, San Diego, CA), p. 62.

Scherer, R. C., Shinwari, D., De Witt, K. J., Zhang, C., Kucinschi, B. R., and Afjeh, A. A. (**2001**). "Intraglottal pressure profiles for a symmetric and oblique glottis with a divergence angle of 10 degrees," J. Acoust. Soc. Am. **109**, 1616–1630.

Stiblar-Martincic, D. (**1997**). "Histology of laryngeal mucosa," Acta Oto-Laryngol., Suppl. **527**, 138–141.

Story, B. H., and Titze, I. R. (**1995**). "Voice simulation with a body-cover model of the vocal folds," J. Acoust. Soc. Am. **97**, 1249–1260.

Tao, C., and Jiang, J. J. (**2006**). "Anterior-posterior biophonation in a finite element model of vocal fold vibration," J. Acoust. Soc. Am. **120**, 1570–1577.

Tao, C., and Jiang, J. J. (**2007**). "Mechanical stress during phonation in a self-oscillating finite-element vocal fold model," J. Biomech. **40**, 2191–2198.

Tao, C., Jiang, J. J., and Zhang, Y. (**2006**). "Simulation of vocal fold impact pressures with a self-oscillating finite-element model," J. Acoust. Soc. Am. **119**, 3987–3994.

Titze, I. R. (**2006**). *The Myoelastic Aerodynamic Theory of Phonation* (National Center for Voice and Speech, Denver, CO), p. 84.

Titze, I. R., and Strong, W. J. (**1975**). "Normal modes in vocal cord tissues," J. Acoust. Soc. Am. **57**, 736–744.

Zhang, K., Siegmund, T., and Chan, R. W. (**2006**). "A constitutive model of the human vocal fold cover for fundamental frequency regulation," J. Acoust. Soc. Am. **119**, 1050–1062.